



Analysing the influence of growing conditions on both energy load and crop yield of a controlled environment agriculture space

Marie-Hélène Talbot^{*}, Danielle Monfet

École de Technologie Supérieure, 1100 Rue Notre-Dame Ouest, Montreal H3C 1K3, Quebec, Canada

HIGHLIGHTS

- Energy and yield of a vertical farm are modelled with TRNSYS for several conditions.
- The influence of temperature, VPD and PPFD were assessed for over 180 scenarios.
- An air temperature of 24 °C represents a better compromise compared to 20 °C or 28 °C.
- Lowering PPFD and extending photoperiod benefit both energy and yield.
- Changing the growing conditions can reduce the need for dehumidification.

ARTICLE INFO

Keywords:

Controlled agriculture environment (CEA)
Vertical farm
Energy modelling
Energy efficiency
Energy load

ABSTRACT

Controlled environment agriculture, such as vertical farming, consists of stacking crops in a controlled environment and is transforming agriculture by providing a highly productive solution for year-round production. However, vertical farms are also energy-intensive due to precise control of the growing conditions (temperature, humidity, carbon dioxide, and lighting). While many studies focus on optimising indoor conditions to enhance yield, the impact of those growing conditions on energy is often overlooked. This study aims to provide a comprehensive analysis, using a dynamic model, of the influence of growing conditions typically used to cultivate lettuces on energy and crop yield. Several combinations of air temperatures (20, 24 and 28 °C), vapour pressure deficits (0.54 and 0.85 kPa), lighting intensities (200 to 700 $\mu\text{mol}\cdot\text{m}^{-2}\cdot\text{s}^{-1}$) and photoperiods (12 to 24 h) are studied. The dynamic model, developed using a building performance simulation tool, supports the simultaneous assessment of energy load and crop yield. It includes a model of a small-scale vertical farm that integrates a dynamic crop model to estimate heat gains/losses from crops and crop growth rate according to growing conditions. The results indicated that the best compromise between energy load and yield is at an air temperature of 24 °C. Moreover, lowering lighting intensity and extending the photoperiod positively impacted both energy load and yield. Certain growing conditions, such as lowering the vapour pressure deficit, can reduce the need for dehumidification. Additionally, for lighting intensities exceeding 500 $\mu\text{mol}\cdot\text{m}^{-2}\cdot\text{s}^{-1}$, although the energy load continued to increase linearly with the lighting intensity, the growth rate was limited, resulting in reduced production efficiency. These extensive results and thorough analyses offer valuable insights into the influence of the growing conditions on energy load and yield.

1. Introduction

The vertical farming industry is experiencing rapid global expansion, with the market projected to surpass four times its 2022 value of USD 5.6 billion by 2030 [1]. This remarkable growth is primarily attributed to advancements in light-emitting diode (LED) technology, which has become more affordable [2]. As a result, research in vertical farming,

also known as plant factories, indoor farms, container farms, and indoor plant environments, has proliferated. The number of journal articles explicitly focusing on vertical farming has significantly increased, growing from less than 175 publications before 2015 to more than seven times that number as of October 2023.

Vertical farming is notorious for its high energy use, spurring a notable increase in energy efficiency, utilisation, and conservation

^{*} Corresponding author.

E-mail address: marie-helene.talbot.1@ens.etsmtl.ca (M.-H. Talbot).

research. Before 2015, only five publications focused on these aspects while reaching nearly fifteen times that number as of October 2023. The energy consumption is mainly attributed to electric lighting and heating, ventilation and air conditioning (HVAC) systems [3]. It is driven by internal loads, mainly attributed to lighting and crops. It has been assessed that, if well insulated, vertical farms' energy consumption is "largely insensitive to location" [4], which means that the outdoor environment has no significant impact on energy consumption. Thus, the main energy consumption for HVAC systems comes from cooling and dehumidification equipment, which are required to dissipate the heat generated by electric lighting and crop transpiration. The cooling and dehumidification equipment ensure the specified indoor air temperature and relative humidity are maintained [5]. The choice of indoor air conditions can substantially influence the energy consumption of the space; in buildings, increasing the cooling setpoint from 22.2 °C to 25 °C has been shown to lead to average savings in cooling energy up to 29% [6]. In parallel, the choice of indoor conditions also influences growth rate.

The growth rate is affected by indoor air conditions, defined by the temperature, humidity, or vapour pressure deficit (VPD). It is also affected by lighting intensity and CO₂ concentration, which, above a specific limit, can reach a saturation point. The VPD, which is the difference between the theoretical pressure exerted by water vapour held in saturated air at a given temperature and the pressure exerted by the water vapour held in the air at the same given temperature, is particularly important. It requires maintaining the air temperature and the humidity level within an acceptable range. Failure to do so can lead to water stress or promote mould growth and diseases, substantially reducing the growth rate or resulting in complete crop loss. Recent crop research has been focused mainly on exploring innovative cultivation techniques and the impact of different indoor environmental conditions to increase yield without compromising nutritional quality. For each crop, and even among different cultivars, optimal growing conditions exist that enhance crop yield in terms of both quality and quantity.

For instance, Carotti et al. [7] investigated the impact of different photosynthetic photon flux densities (PPFD), indoor air conditions and root temperatures on lettuce growth. They maintained the CO₂ concentration at 1200 ppm, the VPD during the photoperiod and dark period at 0.58 kPa and 0.34 kPa, respectively and a photoperiod of 16 h. Table 1 summarises the number of days per cultivation cycle and the production intensity (yield per unit of cultivated area) to produce a 250 g lettuce head of *Lactuca sativa* cv. *Batavia Othilie* for different indoor conditions. Depending on the PPFD level (200, 400, and 750 μmol m⁻²s⁻¹) and indoor air temperature (20, 24, and 28 °C), the cultivation cycle varied between 18 and 28 days. According to the reported data, the yield increased with PPFD and temperature, with the highest yield at 24 °C.

The data reported by Carotti et al. [7] are limited to a fixed CO₂ concentration and photoperiod duration. Other researchers have extensively investigated the impact of CO₂ enrichment, and it has been reported that it can improve productivity by 35% [8]. Jung et al. [9] conducted an experiment on *Lactuca sativa* L. growing in a vertical farm. Their results indicated that a saturation point is reached at a specific CO₂ concentration; beyond that threshold, increasing the CO₂ concentration no longer notably enhances productivity. This saturation point varies depending on factors such as the stage of growth and the growing conditions. Thus, setting the CO₂ concentration to 1200 ppm ensures that CO₂ is not limiting growth. Regarding the impact of photoperiod

duration, Jin, Formiga Lopez, Heuvelink, and Marcelis [10] have reported that crop yield increases linearly for PPFD below 500 μmol•m⁻²•s⁻¹. Similar to CO₂ concentration, saturation can be reached beyond a certain threshold, depending on factors such as the growing conditions. The impact of different combinations of PPFD and photoperiod while maintaining a constant daily light integral (DLI) has also been investigated [11,12]. It was found that for DLI exceeding 10.4 mol•m⁻²•d⁻¹, extending the photoperiod and decreasing the PPFD led to improved yields.

Crop growth also influences the energy use associated with lighting and HVAC systems. As crops grow, their leaves expand, increasing the Photosynthetically Active Radiation (PAR) intercepted and absorbed by crops. This rise in absorbed radiative energy, through photosynthesis, translates into increased crop transpiration, i.e., the latent heat gain from crops. Consequently, as the crops grow, the latent load increases [13], which necessitates more dehumidification to remove the humidity generated by the crops [14]. Moreover, depending on the growing conditions, the leaf temperature is often lower than the air temperature, resulting in the cooling of the air surrounding the crops, which is defined as the sensible heat loss from crops. During the dark period, crops continue to transpire and cool their surroundings, and this effect increases as the leaves expand during growth. Although the humidity setpoint is generally set high, reaching around 85% and 90% during the photoperiod and dark period, respectively [7], dehumidification remains crucial to prevent condensation on colder surfaces, such as the crops leaves, and to mitigate mould growth and diseases. Those phenomena highlight how the choice of growing conditions influences the heat gains/losses from crops, thus indirectly impacting the energy consumption of the space.

Although the influence of growing conditions on yield is well-documented, their influence on both energy consumption and yield is not extensively studied. Consequently, only a few studies have reported energy consumption and yield specifically for lettuce cultivation in vertical farms. As such, Ohyama, Yamaguchi, and Enjoji [15] and Blom, Jenkins, Pulselli, and van den Dobbelen [16] are among the few that have measured energy consumption of the lighting and HVAC equipment, as well as fresh yield. Conversely, several studies have estimated both the energy consumption and fresh yield of lettuces using energy modelling [3,4,17,18] or adopted a mixed approach using measured fresh yield combined with an energy model [19] or simplifications to estimate the energy consumption [20]. The data for annual energy intensity, production intensity, and energy consumption per fresh yield, which can be referred to as the specific energy consumption (SEC), are provided in Table 2. These data are based on the energy consumption of lighting and HVAC equipment for specific indoor conditions, cultivation areas, and fresh yield.

Various factors contribute to the observed disparities, including the growing conditions, the lighting and HVAC equipment design, particularly the photosynthetic photon efficacy (PPE) and the coefficient of performance (COP) of the cooling and dehumidification equipment. Moreover, the selected modelling approach and assumptions are also influential for the modelled results.

The energy intensity ranges from 400 kWh•m⁻² to 1260 kWh•m⁻², being primarily influenced by the combination of PPFD (140 to 500 mol•m⁻²•s⁻¹), photoperiod (12 to 24 h) and PPE (1.5 to 3.5 μmol•J⁻¹). Furthermore, certain results are based on minimal or no dehumidification energy consumption, leading to lower energy intensity. For instance, Graamans et al. [3] and Eaton et al. [21] used floating

Table 1

Cultivation cycle and yield from Carotti et al. [7] to produce 250 g lettuce head with a photoperiod of 16 h under different indoor air conditions.

PPFD (μmol m ⁻² •s ⁻¹)	200			400			750		
Temperature (°C)	20	24	28	20	24	28	20	24	28
Cultivation cycle (days)	28.0	25.3	27.0	21.2	19.0	23.6	18.3	18.1	21.2
Production intensity (kg _{FW} m ⁻²)	81	90	84	108	120	97	125	126	108

Table 2

Reported annual energy intensity, production intensity and SEC based on the energy consumption of lighting and HVAC equipment, cultivation area and fresh yield.

Reference	Type of results ¹	$T_{a,i}$ ² , °C	$\varphi_{a,i}$ ² , %	PPFD, $\mu\text{mol}\cdot\text{m}^{-2}\cdot\text{s}^{-1}$	Photo period, hrs	Production intensity, $\text{kg}\cdot\text{m}^{-2}$	Energy intensity, $\text{kWh}\cdot\text{m}^{-2}$ (%Light/%HVAC) ³	SEC, $\text{kWh}\cdot\text{kg}^{-1}$ ($\text{MJ}\cdot\text{kg}^{-1}$)
Graamans et al. [3]	M	24–30	65–90	500	16	126	1224–1249 (84–93/7–16)	15.5–15.6 (55.8–56.1)
Ohyama et al. [15]	E	24	No setpoint	120/200	15	31	588 (N/A) ⁴	18.7 (67.3)
Zhang and Kacira [18] - low DLI	M	24	No setpoint	226	16	57–58	416–439 (86–90/10–14)	7.1–7.7 (25.6–27.2)
Zhang and Kacira [18] - high DLI				260		63	484–527 (82–90/10–18)	7.7–8.3 (27.2–30.0)
Blom et al. [16]	E	N/A ⁴	N/A ⁴	140	20	69	1020 (66/34)	14.8 (53.3)
Talbot et al. [17]	M	21	70	434	12	61	1092 (52/48)	18.0 (64.8)
Blom et al. [19]	M	24	79	200	16	79	418 (80/20)	5.3 (19.1)
Eaton et al. [21] - reference	M	19–24	50–85	200	24	104	1259 (69/31)	12.2 (43.9)
Eaton et al. [21] - optimised							640 (70/30)	6.2 (22.3)
Stanghellini and Katzin [20]	M	24	80	200	16	91	400 (80/20)	4.4 (15.8)

¹ M: Modelling, E: Experimental.² $T_{a,i}$: Indoor air temperature | $\varphi_{a,i}$: Indoor air relative humidity.³ Percentage of electricity associated with electric lighting (%Light) and HVAC equipment (%HVAC).⁴ N/A: Not available.

humidity setpoints, while Zhang and Kacira [18] did not specify any humidity setpoint. Given the high energy requirement for dehumidification, a model that tightly controls temperature and humidity will likely exhibit higher energy intensity. This aligns with experimental findings. For example, Ohyama et al. [15] reported a much lower energy intensity of $588 \text{ kWh}\cdot\text{m}^{-2}$ in their vertical farm compared to $1020 \text{ kWh}\cdot\text{m}^{-2}$ in the study by Blom et al. [16], despite having similar PPFD and photoperiod. Indeed, Ohyama et al. [15] had no humidity control and a PPE of $2.9 \mu\text{mol}\cdot\text{J}^{-1}$, while Blom et al. [16] results included the use of an independent dehumidification system and a low PPE of $1.5 \mu\text{mol}\cdot\text{J}^{-1}$. The only exception among the studies reported in Table 2 is the model from Blom et al. [19], which has a low energy intensity of $418 \text{ kWh}\cdot\text{m}^{-2}$. This is explained by the HVAC equipment that cools and dehumidifies indoor air, a single packaged air handling unit with an overall COP of 3.6. Single packaged air handling units are far more efficient than conventional systems, like split cooling units combined with independent dehumidifiers, as modelled by Talbot et al. [17] and Eaton et al. [21]. Also, the annual energy intensity estimated by Blom et al. [19] did not include the energy consumption during the dark photoperiod, for which dehumidification is usually needed.

The production intensity ranges from $31 \text{ kg}_{\text{FW}}\cdot\text{m}^{-2}$ to $126 \text{ kg}_{\text{FW}}\cdot\text{m}^{-2}$, primarily influenced by the crop growth rate, planting crop density and the weight of harvested lettuce head. The median production intensity reported is $66 \text{ kg}_{\text{FW}}\cdot\text{m}^{-2}$, which is relatively low, as it has the potential to reach at least $90 \text{ kg}_{\text{FW}}\cdot\text{m}^{-2}$ and theoretically go up to $190 \text{ kg}_{\text{FW}}\cdot\text{m}^{-2}$ [19] for a planting crop density of $25 \text{ plants}\cdot\text{m}^{-2}$, a harvested weight of 250 g, and given the growing conditions outlined by Carotti et al. [22]. The results suggest that the growing conditions used by Ohyama et al. [15] and Blom et al. [16] may have limited growth; notably, Blom et al. [16] did not have any CO_2 enrichment system.

The energy consumption per fresh yield, the SEC, is the main indicator used to assess and improve energy efficiency. Most SEC reported in the literature are derived from energy models, while a minority are based on experimental results or survey data from operational facilities [23]. The SEC ranges from 4.4 to $18.7 \text{ kWh}\cdot\text{kg}_{\text{FW}}^{-1}$ of fresh weight, indicating a considerable variation, which is even more pronounced when considering various crops, with SEC ranging from 3.2 to $59.1 \text{ kWh}\cdot\text{kg}_{\text{FW}}^{-1}$ [4,24,25]. Although SEC is a widely used indicator for assessing vertical farming energy efficiency, it may be insufficient. Two

facilities could have similar SEC values yet have significantly different production intensities.

Among the studies that have reported numerical results in Table 2, differences in the modelling approach were observed. Regarding growth modelling, most studies used Van Henten's model [26], which has been validated for semi-closed greenhouses but might not be suitable for vertical farms in its original form [3,27]. Blom et al. [19] did not model growth and instead relied on experimental data to estimate yield. This approach lacks the versatility to assess energy consumption and yield under different growing conditions, as it would require conducting experiments for each set of conditions. Regarding energy modelling, most studies assumed the heat gains/losses from crops remained constant, overlooking their variation as the lettuces grew. In most cases, the modelling approaches for energy and growth were decoupled. This means most of the study neglected the indirect influence of growing conditions and that the growth model was only used to estimate yield.

To balance energy consumption and yield in vertical farms, it is essential to grasp the influence of growing conditions on both energy consumption and yield. Given the many possible combinations of parameters, comparing existing studies and understanding how growing conditions influence energy consumption and yield is challenging for several reasons. Each study has focused on a specific set of conditions, while numerous combinations of growing conditions (e.g., air temperature, VPD, PPFD, photoperiod, CO_2 concentration) are possible. Moreover, the combinations selected generally resulted in low productivity intensity, which hinders understanding the influence of growing conditions on the energy efficiency of highly productive vertical farms. Additionally, some studies did not consider highly influential factors, such as CO_2 enrichment, precise control of temperature and humidity, and the implementation of the dehumidification systems typically found in vertical farms. Furthermore, the energy consumption during the dark period must be included in the calculation, as it is not negligible. Comparing studies is also challenging due to significant variations in HVAC and lighting systems, including the type of equipment, the COP of the equipment, and lighting efficacies. Consequently, analysing the results from these studies and determining how the growing conditions influence energy efficiency in vertical farms is complex. Thus, for vertical farms, the influence of growing conditions on energy consumption and yield remains sparsely documented. Furthermore, ongoing research

should aim to identify the best combination of growing conditions for vertical farms, including the corresponding impact on energy load, according to the space energy balance. This approach offers more insightful results than solely energy consumption assessment, which is influenced by the performance of HVAC equipment [24]. Clear conclusions remain elusive, necessitating further research to simultaneously investigate the influence of the growing conditions on energy load and yield, which requires a dynamic modelling approach tailored for vertical farms.

This study aims to bridge this gap by completing a comprehensive parametric analysis of growing conditions and their influence on energy load and yield of a small-scale vertical farm, a high-density controlled environment agriculture (CEA) space. The selected growing conditions cover many real-world possibilities, including combinations that result in high productivity intensities. The analysis uses a transient modelling approach that integrates a dynamic crop model adapted to vertical farming applications to estimate (1) the heat exchanges between the crops and their environment while crops grow and (2) yield. The objective is to gain a deeper understanding of the energy requirements and their sensitivity to growing conditions, all while considering the influence of these growing conditions on crop yield.

2. Methodology

This paper aims to evaluate the influence of growing conditions on the energy load and yield of high-density CEA spaces. The selected approach estimates the energy load and yield using a crop growth model for growing scenarios using a high-density CEA space model created in a building performance simulation (BPS) tool. The scenarios result from all possible combinations of several growing conditions, and the energy load is calculated based on the space energy demand, excluding HVAC equipment.

The design and operation of high-density CEA spaces are challenging and require complex HVAC equipment to meet the grower’s operation requirements. High-density CEA spaces, commonly referred to as vertical farms, are usually airtight and thus include two main sources/sinks of heat: the gains from lighting and the gains/losses from crops [28]. Lights and crops induce significant loads, leading to high energy loads in electricity, cooling and dehumidification. Energy modelling can assist the design and operation of energy-efficient CEA spaces. Two different

approaches are proposed in the literature. The first one consists of using programming software (e.g., MATLAB), and the second one is using BPS tools (e.g., EnergyPlus, TRNSYS, etc.). BPS tools offer many advantages since they are used for different building applications. These advantages include meteorological data availabilities for several weather stations that are easy to use as inputs, thermal exchanges that are modelled according to well-established formulations, and extensive libraries of equipment. Creating a building model with a BPS tool is thus much faster and less prone to errors than developing a new script written from scratch in programming software. Hence, several researchers prefer using a BPS tool to model agricultural spaces such as greenhouses, plant factories or building integrated agricultural spaces to assess the space energy demand and HVAC energy end use [29]. Co-simulation is sometimes chosen to model the space and crops using two tools [30].

Crops have been included in models of agricultural spaces to estimate energy load and crop yield to improve the analysis of CEA spaces. This involves modelling the heat exchanges of crops with their environment, referred to as the “airnode” in most BPS tools, including latent heat gains, sensible heat gains or losses and light interception. Fig. 1 illustrates some heat exchanges in a vertical farm, highlighting the close interaction between lighting and crops. Lighting influences the magnitude of the heat gains/losses from crops, and as the crops grow, the heat gains from lighting decrease due to light interception.

Thus, several thermal phenomena must be modelled to estimate the load, which includes the electric energy demand for lighting as well as the rate of sensible and latent heat to be removed or added to maintain a constant room air temperature and humidity level.

2.1. Description of the model

The high-density CEA space model, the vertical farm, was created in TRNSYS [31] and included three main components: electric lighting, crops, and a thermal zone. Fig. 2 illustrates the interactions between these components and the flow of variables between them and also provides a visual representation of the model’s inputs and outputs. The dynamic crop model includes an energy balance and a growth model to estimate the heat exchanges between crops and their environment as they grow [27]. The high-density CEA model has been previously validated using numerical results from Graamans et al. [5]: the differences in energy load intensities were 0%, 5% and 1% for lighting, cooling and

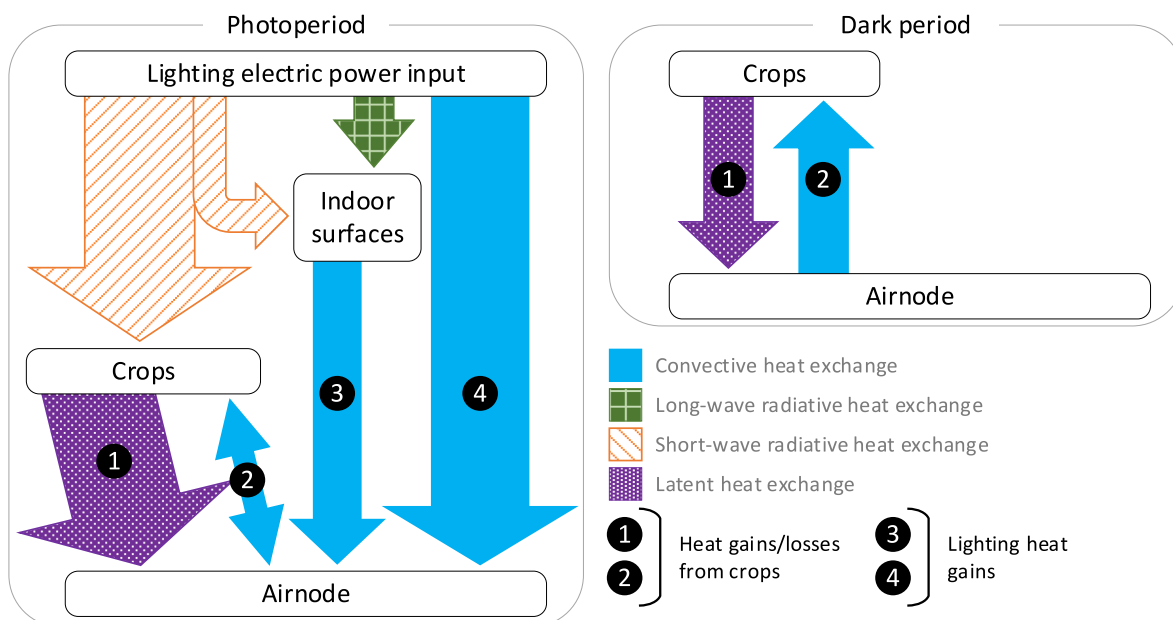


Fig. 1. Visualization of the heat exchanges that occur between lights, crops, indoor surfaces and the airnode within a CEA space.

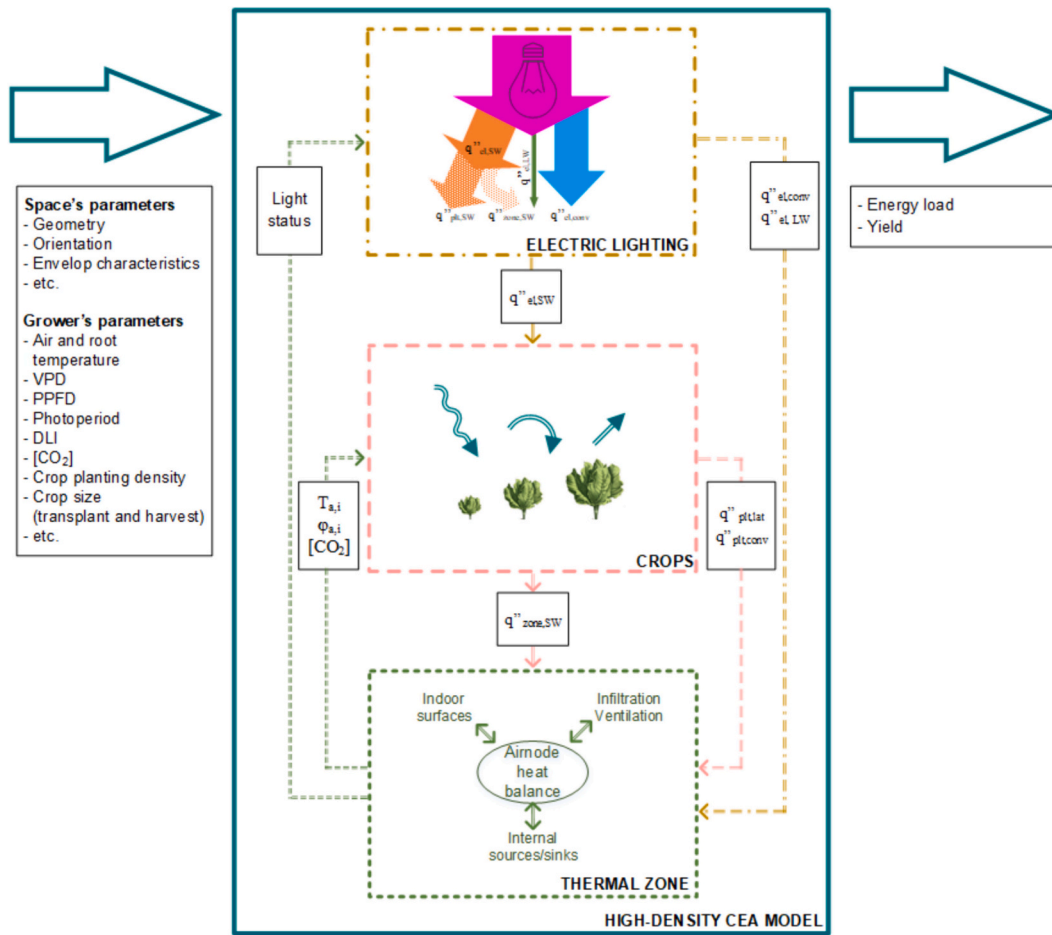


Fig. 2. Overview of the model.

dehumidification, respectively [21].

The thermal zone model includes gains/losses from the electric lighting component and the crop model. The electric lighting component divides the associated heat gain in three main gains, as also illustrated in Fig. 1: the convective lighting heat gain ($\dot{q}_{el,conv}$), which is sent directly to the thermal zone; the long-wave lighting heat gain ($\dot{q}_{el,LW}$), which is treated as part of the radiative heat gain to the thermal zone; and the photosynthetic active radiation (short-wave radiation) from electric lighting ($\dot{q}_{el,SW}$), which is divided into two parts, one is absorbed by the crops ($\dot{q}_{plt,SW}$) and the other one is computed as a radiative heat gain to the thermal zone ($\dot{q}_{zone,SW}$). For the crop model, at every simulation time step, the indoor air conditions – air temperature ($T_{a,i}$), relative humidity ($\phi_{a,i}$) and carbon dioxide concentration ($[CO_2]$) – and the photosynthetic active radiation (short-wave radiation) from electric lighting ($\dot{q}_{el,SW}$) are used as inputs to estimate the heat gains/losses from crops ($\dot{q}_{plt,lat}$ and $\dot{q}_{plt,conv}$). Those are considered additional internal heat gains/losses to the thermal zone. The model outputs the energy load, which is the sum of the lighting, cooling, dehumidification and heating loads. These correspond to the integral over time of the lighting power input, the rate of sensible heat removal, the rate of latent heat removal and the rate of sensible heat addition. These rates are calculated at each time step to maintain the specified indoor air conditions (temperature and relative humidity) at all times. Each component is further described in Sections 3.1.1. to 3.1.3.

2.1.1. Thermal zone

In high-density CEA spaces, crops grow at high density –stacked vertically or horizontally – and only electric lighting is used. Fig. 3 illustrates the modelled high-density CEA space, which is located in a building maintained at an ambient temperature of 20 °C. The enclosure properties are listed in Table 3. The indoor surfaces are covered with water-repellent panels to minimise water vapour migration through the envelope. The space is enriched in CO₂ to enhance crop growth and is airtight to avoid the dilution of the CO₂. Moreover, it is assumed that the air is well-mixed and air velocity over the leaves is sufficient to facilitate

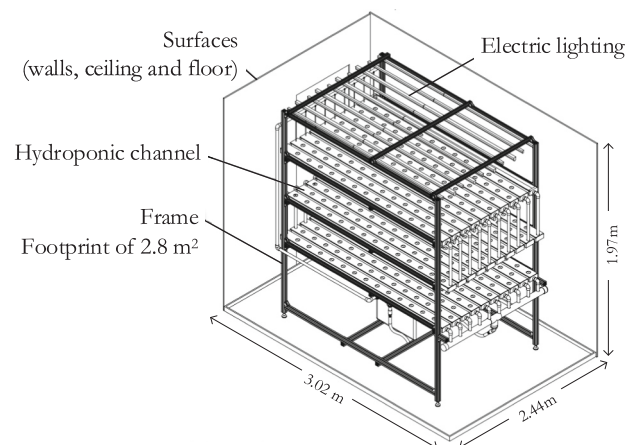


Fig. 3. Small-scale high-density CEA space.

Table 3
Characteristics of the envelope of the high-density CEA space.

U-Value, $W \cdot (K \cdot m^2)^{-1}$	0.12
Thermal capacity, $J \cdot (kg \cdot K)^{-1}$	1000
Density, $kg \cdot m^{-3}$	113.17

gas exchange.

2.1.2. Electric lighting

Growing conditions alternate between two states: (1) photosynthesis that occurs during the photoperiod (when the electric lighting is on) and (2) respiration that occurs during the dark period (when the electric lighting is off). The photoperiod is set to start at 00:00, i.e., the lighting is turned on at 00:00. As previously stated, the electric lighting power input (q_{el}^{\prime}) is split in three: the convective heat gain ($q_{el,conv}^{\prime}$), the long-wave radiation heat gain ($q_{el,LW}^{\prime}$), and the short-wave radiation ($q_{el,SW}^{\prime}$). The latter is divided into two: the radiation absorbed by crops ($q_{plt,SW}^{\prime}$) and the radiation not absorbed by crops ($q_{zone,SW}^{\prime}$), which is computed as a radiative heat gain to the thermal zone. Eqs. (1) to (5) define the electric lighting heat gains, while the main characteristics of the electric lighting are listed in Table 4.

$$q_{el,conv}^{\prime} = f_{conv} \cdot q_{el}^{\prime} \quad (1)$$

$$q_{el,LW}^{\prime} = f_{LW} \cdot q_{el}^{\prime} \quad (2)$$

$$q_{el,SW}^{\prime} = f_{SW} \cdot q_{el}^{\prime} \quad (3)$$

$$q_{plt,SW}^{\prime} = (1 - e^{-k_{s,el} LAI}) \cdot q_{el,SW}^{\prime} \quad (4)$$

$$q_{zone,SW}^{\prime} = q_{el,SW}^{\prime} - q_{plt,SW}^{\prime} \quad (5)$$

where q_{el}^{\prime} is the electric lighting power input ($W \cdot m_{cultivated}^{-2}$); $q_{el,conv}^{\prime}$ is the convective heat gain from electric lighting ($W \cdot m_{cultivated}^{-2}$); $q_{el,LW}^{\prime}$ is the long-wave radiation heat gain from electric lighting ($W \cdot m_{cultivated}^{-2}$); $q_{el,SW}^{\prime}$ is the short-wave radiation flux from electric lighting ($W \cdot m_{cultivated}^{-2}$); $f_{conv}/f_{SW}/f_{LW}$ are the electric lighting heat fractions; $q_{plt,SW}^{\prime}$ is the short-wave radiation flux absorbed by the crops from electric lighting ($W \cdot m_{cultivated}^{-2}$); $k_{s,el}$ is the extinction coefficient associated to PAR from electric lighting; and $q_{zone,SW}^{\prime}$ is the short-wave radiation flux not absorbed by crops from electric lighting ($W \cdot m_{cultivated}^{-2}$). The extinction coefficient, which accounts for the light attenuation in the canopy, depends on the leaf optical properties, the geometry of the crops, and the wavelength of the light.

2.1.3. Crops

The dynamic crop model combines an energy balance and a growth model to estimate the heat exchanges between crops and their environment as they grow. The energy balance is an adaptation of the validated model proposed by Graamans et al. [32], which was adjusted to enhance its versatility [27]. The growth model is an adaptation of the one initially proposed by Van Henten [26], which has been adjusted for high-density CEA application by Talbot and Monfet [27]. As such, certain equations of the original model were revised based on recent

Table 4
Characteristics of the electric lighting.

Lamp type	LED
Photosynthetic photon efficacy (PPE)	2.6 $\mu mol \cdot J^{-1}$
Heat fractions ($f_{conv}/f_{LW}/f_{SW}$)	0.37 / 0.11 / 0.52

literature and four sensitive parameters were calibrated using the experimental dataset from Carotti et al. [22]. Calibration was conducted for nine sets of conditions based on fresh weight per plant, resulting in root mean square error (RMSE) ranging from 2.1 to 18.2 $g_{FW} \cdot plant^{-1}$. It was demonstrated that this calibration led to relative differences in the energy load per fresh weight, the specific energy load, of 0.1% to 3.5% over a growth cycle compared to the specific energy load obtained from the experimental dataset. This last verification ensure that the calibrated model was suitable for energy analysis since it induces reasonable errors. Additionally, the growth model was assessed for its suitability under different lighting intensities compared to those used by Carotti et al. [22], resulting in a satisfactory level of robustness with R-square ranging from 0.86 to 0.92. Details of the growth model and the values of the calibrated parameters are provided in Appendix A. The growth model estimates, at every timestep, the total (shoot and root) plant dry weight (DW_{tot}), the shoot fresh weight (FW_{sh}) and the leaf area index (LAI) for a root temperature equal to air temperature and a constant CO_2 concentration of 1200 ppm. The LAI is defined as the ratio of the total leaf area to the cultivated area and can be estimated by multiplying the crop's leaf area by the planting crop density. The LAI plays a crucial role in the energy balance as it significantly influences some of the heat exchanges within the space, such as:

- the portion of the PAR absorbed by crops ($q_{plt,SW}^{\prime}$) and the associated radiative heat gain from electric lighting ($q_{zone,SW}^{\prime}$) estimated according to Eqs. (4) and (5), respectively;
- the heat gains/losses from crops as the leaves grow, more specifically the crops latent heat gain ($q_{plt,lat}^{\prime}$) and crops sensible heat gain/loss ($q_{plt,conv}^{\prime}$) estimated using Eqs. (6) and (7), respectively.

$$q_{plt,lat}^{\prime} = LAI \cdot \lambda \frac{\chi_s - \chi_a}{r_s + r_a} \quad (6)$$

$$q_{plt,conv}^{\prime} = LAI \cdot \rho_{a,i} \cdot c_{p,a,i} \frac{T_{plt} - T_{a,i}}{r_a} \quad (7)$$

where $q_{plt,lat}^{\prime}$ is the crops latent heat gain ($W \cdot m_{cultivated}^{-2}$); $q_{plt,conv}^{\prime}$ is the crops convective heat gain or loss; LAI is the Leaf Area Index ($m_{leaves}^2 \cdot m_{cultivated}^{-2}$); λ is the heat of vaporisation of water ($kJ \cdot kg^{-1}$); χ_s is the vapour concentration at the canopy level ($g \cdot m^{-3}$); χ_a is the air vapour concentration ($g \cdot m^{-3}$); r_s is the stomatal resistance ($s \cdot m^{-1}$); r_a is the aerodynamic resistance ($s \cdot m^{-1}$); $\rho_{a,i}$ is the indoor air density ($kg \cdot m^{-3}$); $c_{p,a,i}$ is the specific heat of the indoor air ($J \cdot (kg \cdot K)^{-1}$); T_{plt} is the leaves temperature ($^{\circ}C$); and $T_{a,i}$ is the indoor air temperature.

2.2. Growing conditions

The selected growing conditions cover various growing conditions, including different dry bulb air temperature setpoints, VPD setpoints and lighting intensities. Each combination of these growing conditions represents a scenario wherein the energy load of the space and crop yield is estimated. The CO_2 concentration and VPD during the dark period are set at 1200 ppm and 0.48 kPa for all growing conditions. Also, the root temperature is equal to the air temperature, the crop planting density is 25 $crops \cdot m^{-2}$, the transplant weight is fixed at 1.2 $g_{FW} \cdot plant^{-1}$, and the harvested weight is specified as the maximum marketable weight of 250 $g_{FW} \cdot plant^{-1}$.

2.2.1. Air temperature and vapour pressure deficit (VPD)

Air temperature influences energy load, heat gains/losses from crops and crop growth, while VPD influences energy load and heat gains/losses from crops. Table 5 tabulates the selected temperatures and their corresponding relative humidity for the photoperiod/dark period, which vary according to the VPD setpoint. The temperature range is set between 20 $^{\circ}C$ (lower limit) and 28 $^{\circ}C$ (upper limit) based on experimental

Table 5

Air temperature and associated relative humidity for a constant VPD maintained during photoperiod/dark period of 0.54/0.48 kPa and 0.85/0.48 kPa.

Air temperature, °C	Relative humidity (photoperiod / dark period), %	
	VPD of 0.54 / 0.48 kPa	VPD of 0.85 / 0.48 kPa
20	77 / 79	64 / 79
24	82 / 84	71 / 84
28	86 / 87	77 / 87

data reported by Carotti et al. [22]. Additionally, the VPD for the photoperiod and dark period, with a VPD range during the photoperiod of 0.54 kPa (lower limit) and 0.85 kPa (upper limit), are specified in Table 5.

2.2.2. Photosynthetic photon flux density (PPFD)

PPFD influences energy load, heat gains/losses from crops, crop growth and lighting heat gains. Table 6 tabulates the selected PPFD and their corresponding DLI for photoperiods of 12-, 14-, 16-, 18-, 20- and 22-h. The PPFD range of 200 to 700 $\mu\text{mol}\cdot\text{m}^{-2}\cdot\text{s}^{-1}$ is based on experimental data from Carotti et al. [22]. A photoperiod of 24 h is not considered because both Pennisi et al. [33] and Silva et al. [34] suggested that the optimal photoperiod for lettuce might be shorter than 24 h. Silva et al. [34] observed that at a PPFD of 400 $\mu\text{mol}\cdot\text{m}^{-2}\cdot\text{s}^{-1}$, continuous light significantly hindered lettuce growth and led to the lowest lighting energy efficiency compared to photoperiods of 12 to 22 h. Moreover, the number of scenarios is limited by the use of DLI ranging from 11.5 to 43.2 $\text{mol}\cdot\text{m}^{-2}\cdot\text{day}^{-1}$ as reported by Carotti et al. [22].

The combination of all these growing conditions results in 180 scenarios, as illustrated in Fig. 4.

3. Results

Annual simulations are completed for each of the 180 scenarios to compile data on the space energy demand, the associated energy load, the energy load per category and crop yield. Fig. 5 displays the annual crop yield and energy load for all scenarios (Fig. 4), with distinct symbols for photoperiods. The results unveil disparities in annual energy load and crop yield, ranging from 35 to 98 GJ and 560 to 1631 kg_{FW} , respectively. Moreover, the specific energy load, which assesses the efficiency of the production process, varied between 37.0 and 117.8 $\text{MJ}\cdot\text{kg}_{\text{FW}}^{-1}$. The results illustrate indoor environment conditions' significant influence on energy load and crop yield. The energy load increases linearly with crop yield as the duration of the photoperiod increases. Notably, the slope of this linear regression consistently steepens with higher PPFD, indicating that the trade-off between yield and energy load is declining at high PPFD.

The energy load per category averaged over the temperature for scenarios with a VPD of 0.54 kPa is illustrated in Fig. 6. For those scenarios, the main energy load is for lighting, which accounts for 42–50% of the energy load. Meanwhile, cooling, dehumidification and heating contribute to 23–35%, 14–26% and 1–9% of the energy load, respectively.

A separate analysis of the growing conditions is conducted to

Table 6

Resulting DLI ($\text{mol}\cdot\text{m}^{-2}\cdot\text{day}^{-1}$) values for PPFD of 200 to 700 $\mu\text{mol}\cdot\text{m}^{-2}\cdot\text{s}^{-1}$ combined to a photoperiod of 12-, 14-, 16-, 18-, 20- and 22-h.

Photoperiod, hrs PPFD, $\mu\text{mol}\cdot\text{m}^{-2}\cdot\text{s}^{-1}$	12	14	16	18	20	22
200	–	–	11.5	13.0	14.4	15.8
300	13.0	15.1	17.3	19.4	21.6	23.8
400	17.3	20.1	23.0	25.9	28.8	31.7
500	21.6	25.2	28.8	32.4	36.0	39.6
600	25.9	30.2	34.6	38.9	43.2	–
700	30.2	35.3	40.3	–	–	–

understand better the disparities observed in the results depicted in Fig. 5. This analysis assesses the influences of each growing condition category on energy load and crop yield.

3.1. Air temperature

The influence on the energy load using lower (20 °C) or higher temperature (28 °C) setpoints, with 24 °C as the reference, is illustrated in Fig. 7.

The most significant reduction in energy load due solely to changes in air temperature occurs at the lowest PPFD, gradually decreasing with higher PPFD. Moreover, the reduction is more critical at high VPD than at low VPD. At a VPD of 0.85 kPa, when temperatures are set to 20 °C and 28 °C, the maximum reductions are 13% and 10%. When PPFD reaches 500 and 700 $\mu\text{mol}\cdot\text{m}^{-2}\cdot\text{s}^{-1}$, reductions below 2% are observed, whether under low or high VPD. This highlights that for high PPFD, the influence of the air temperature on energy load becomes less significant, i.e., the energy load is driven by the lighting and the required cooling rather than dehumidification.

Regarding the energy load per category, lowering the air temperature to 20 °C increases the cooling load. The overall decrease in energy load is attributed to lower dehumidification and heating loads. This is explained by lower heat gains/losses from crops at 20 °C. The heat gains/losses from crops peak at 24 °C, leading also to a reduction in energy load when the air temperature is raised to 28 °C. When the air temperature is raised to 28 °C, one would expect a decrease in cooling load due to the higher air temperature. Surprisingly, the results show an increase in cooling load. This is attributed to the heat gains/losses from crops: the crops cool their surroundings to a lesser extent at 28 °C than at 24 °C, mitigating the reduction in cooling demand expected for a higher air temperature setpoint. This dampens the benefit of raising the temperature to reduce the cooling load. Considering all those complex interactions, a more significant reduction is consistently achieved when the air temperature changes to 20 °C rather than 28 °C. The scenarios at 24 °C consistently exhibit the highest dehumidification load per fresh yield.

Crop yield is also reduced by changes in air temperature to 20 °C or 28 °C, ranging from 11% to 27%. The combined reduction in energy load and crop yield increases specific energy load, as illustrated in Fig. 8, ranging from 1% to 35%. Thus, when considering energy load and crop yield simultaneously, maintaining the temperature at 24 °C is the best option, resulting in the lowest specific energy load, especially at high PPFD. It is worth noting that for scenarios at 200 $\mu\text{mol}\cdot\text{m}^{-2}\cdot\text{s}^{-1}$ and 0.85 kPa, a mere 1% increase is observed when the temperature changes to 28 °C.

3.2. VPD

The influence of using a low VPD (0.54 kPa) on energy load, with a high VPD (0.85 kPa) being considered as the reference, is illustrated in Fig. 9.

Lowering the VPD leads to a higher reduction in energy load at lower PPFD. This reduction is more important at 24 °C, reaching 14%, while it is 9% and 11% for air temperatures of 20 °C and 28 °C, respectively. Reductions of less than 2% are noted for PPFD exceeding 500 $\mu\text{mol}\cdot\text{m}^{-2}\cdot\text{s}^{-1}$ at air temperatures of 20 °C and 28 °C and exceeding 600 $\mu\text{mol}\cdot\text{m}^{-2}\cdot\text{s}^{-1}$ at 24 °C, demonstrating that at high PPFD, the influence of VPD on the energy load becomes negligible.

Regarding the energy load per category, lowering the VPD at low PPFD leads to higher relative humidity, which lowers the dehumidification load and heat gains/losses from crops. The latter results in a slight increase in cooling load. As the PPFD rises, heat gains/losses from crops become more critical. At high PPFD, lowering the VPD reduces the dehumidification load but significantly increases the cooling load. At 700 $\mu\text{mol}\cdot\text{m}^{-2}\cdot\text{s}^{-1}$, the reduction in dehumidification load is entirely offset by the increase in cooling load.

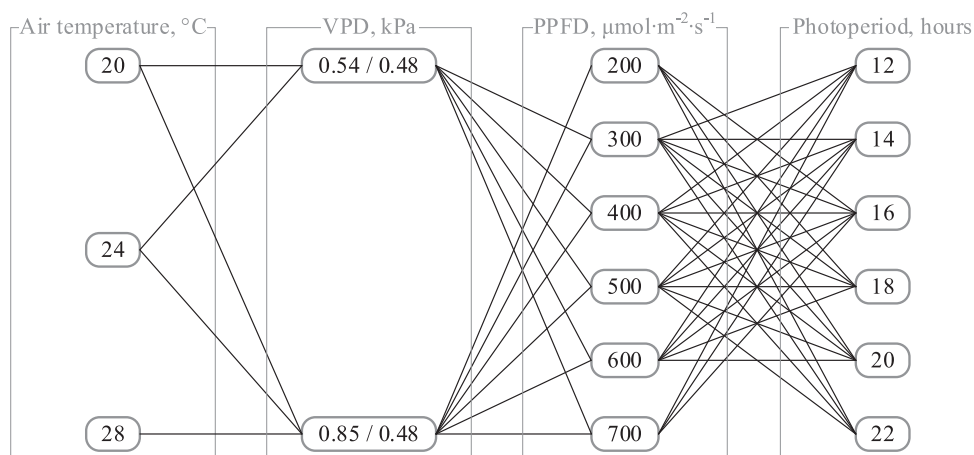


Fig. 4. Representation of the 180 scenarios.

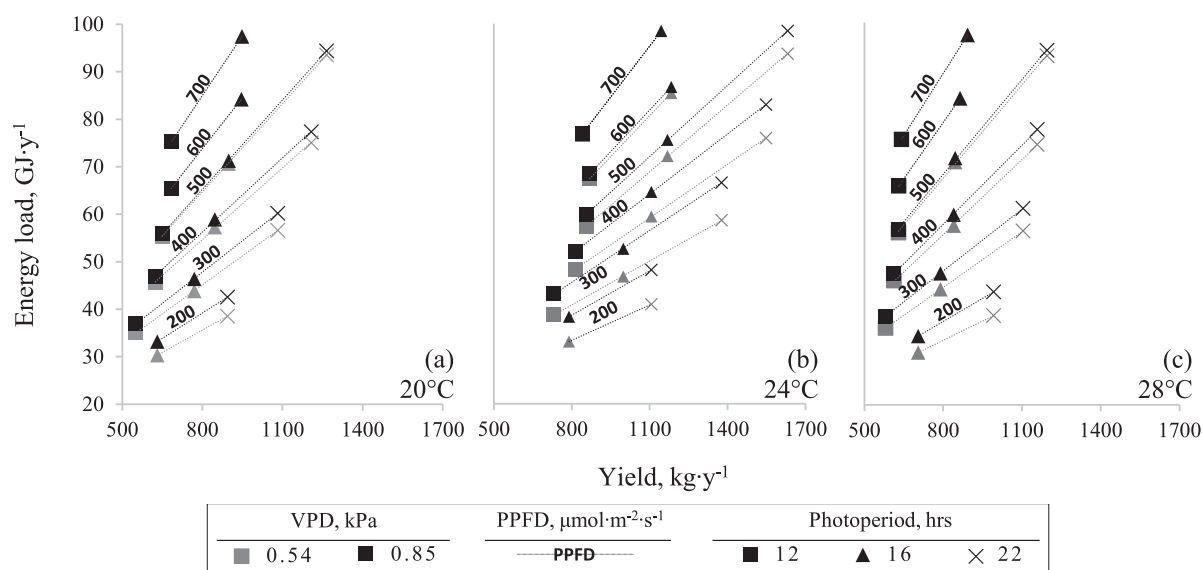


Fig. 5. Annual energy load and yield for scenarios with a photoperiod of 12, 16 and 22 h.

Crop yield is not affected by lowering the VPD since it is assumed that VPDs of 0.54 kPa and 0.85 kPa do not induce water stress and, thus, do not limit crop growth.

3.3. PPFD

When maintaining a constant photoperiod, increasing the PPFD leads to higher lighting and cooling demands due to lighting, resulting in a substantial rise in energy load. The combined energy load for lighting and cooling increases from 50% to 87% with higher PPFD.

Fig. 10 illustrates how energy load and crop yield vary with the PPFD for an air temperature of 24 °C, VPD of 0.54 kPa, and photoperiods of 12 to 22 h. The energy load increases linearly with the PPFD for each photoperiod. Likewise, crop yield increases linearly for PPFD below 500 $\mu\text{mol}\cdot\text{m}^{-2}\cdot\text{s}^{-1}$, which aligns with information reported by Jin, Formiga Lopez, Heuvelink, and Marcelis [10], which was also corroborated in the development of the growth model by Talbot and Monfet [27]. However, beyond 500 $\mu\text{mol}\cdot\text{m}^{-2}\cdot\text{s}^{-1}$, other limiting factors come into play, diminishing production efficiency at high PPFD.

3.4. Yield for different combinations of PPFD/photoperiod for a constant DLI

Additional results are generated at an air temperature of 24°C and VPD of 0.54 kPa to investigate the influence of varying the PPFD while maintaining a constant DLI of 14, 18 and 20 $\text{mol}\cdot\text{m}^{-2}\cdot\text{d}^{-1}$. Table 7 tabulates the selected PPFD and their corresponding photoperiods for DLI of 14, 18, 20, 22 and 24 $\text{mol}\cdot\text{m}^{-2}\cdot\text{d}^{-1}$.

Fig. 11 illustrates how energy load and crop yield vary with the PPFD for an air temperature of 24 °C, VPD of 0.54 kPa, and DLI of 14, 18, 20, 22 and 24 $\text{mol}\cdot\text{m}^{-2}\cdot\text{d}^{-1}$. When PPFD is lowered by 100 $\mu\text{mol}\cdot\text{m}^{-2}\cdot\text{s}^{-1}$ while maintaining a constant DLI, it leads to a modest reduction in energy load of 2 to 7%. Although scenarios with the same DLI have identical lighting loads, reducing the PPFD and extending the photoperiod slightly decrease the cooling, dehumidification and heating loads. Regarding crop yield, extending the photoperiod while maintaining a constant DLI increases crop yield, ranging from 20% to 24%. Lowering the PPFD while extending the photoperiod is particularly interesting as it substantially impacts crop productivity and, to a lesser extent, holds the potential to improve energy load, ultimately improving the specific energy load.

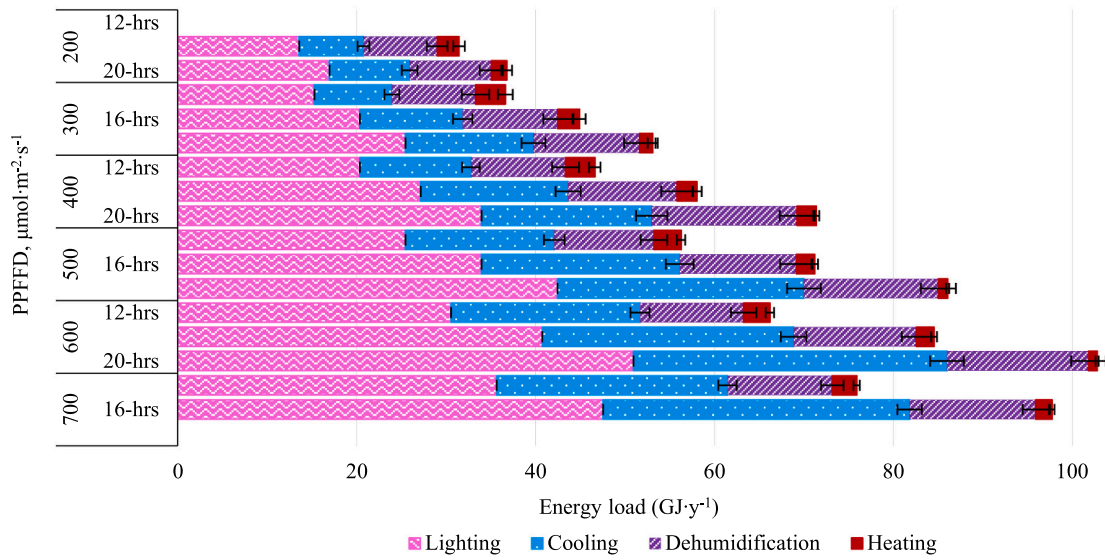


Fig. 6. Energy load per category averaged over the temperature for scenarios with a VPD of 0.54 kPa.

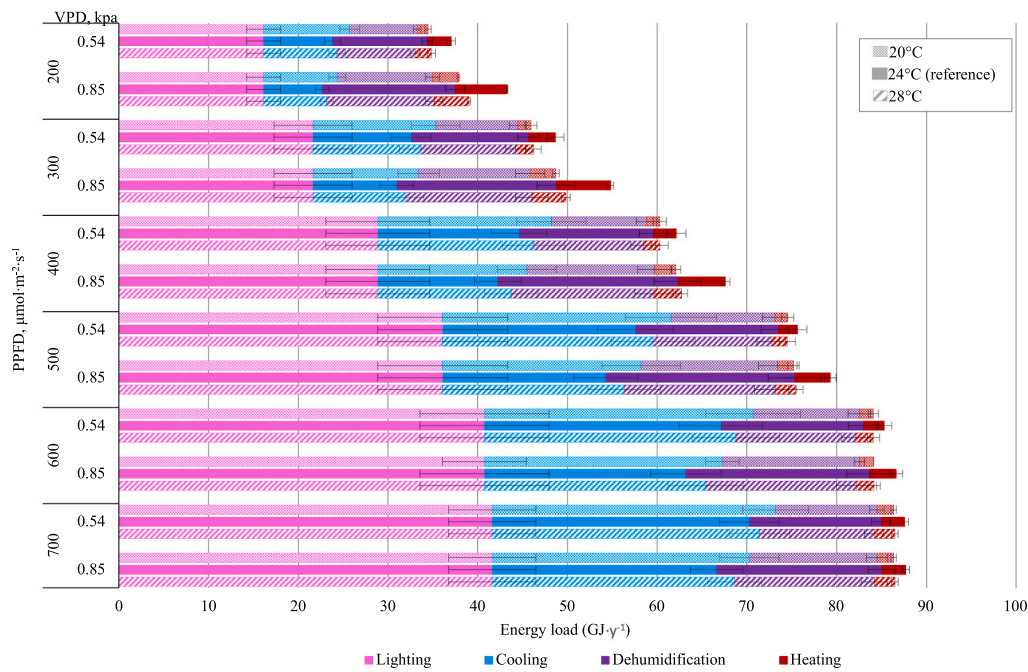


Fig. 7. Energy load per category averaged over the photoperiod for scenarios with an air temperature of 20 °C, 24 °C and 28 °C.

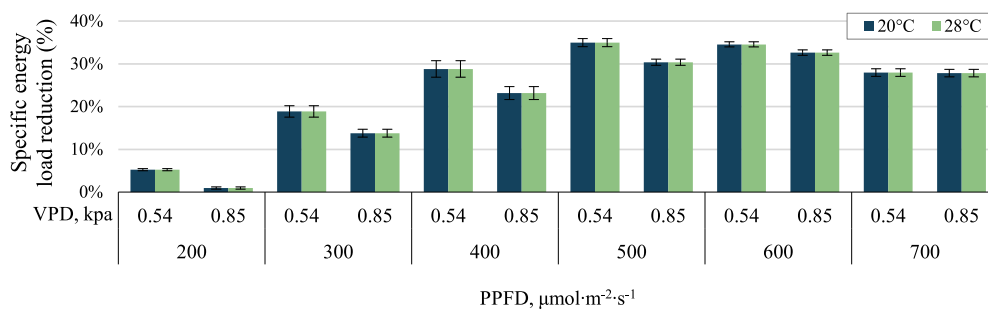


Fig. 8. Reduction in specific energy load resulting from changes in temperature with a reference air temperature of 24 °C.

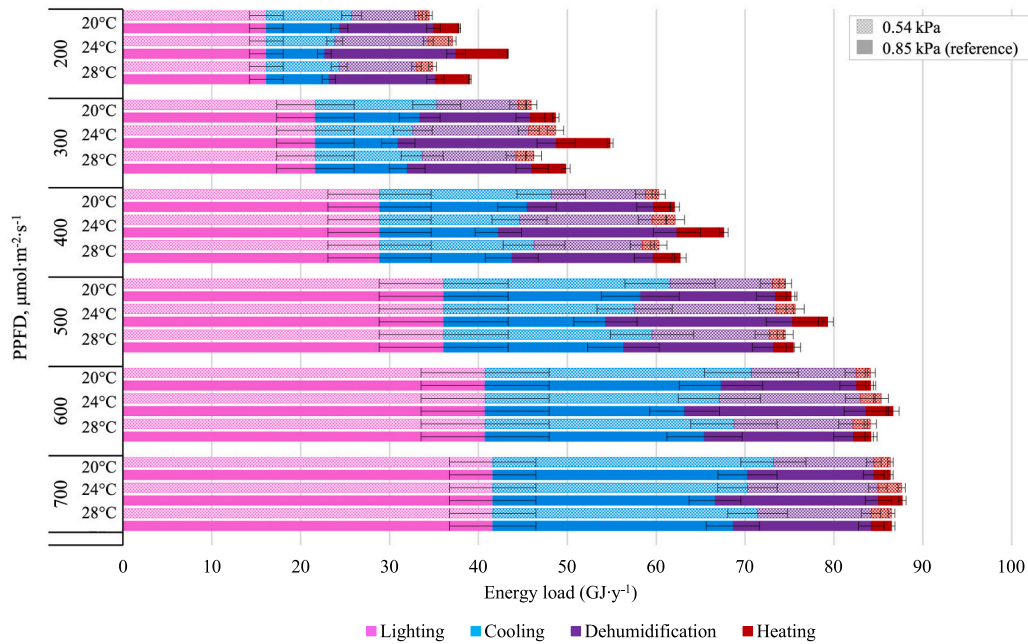


Fig. 9. Energy load per category averaged over the photoperiod for scenarios with a VPD of 0.54 kPa and 0.85 kPa.

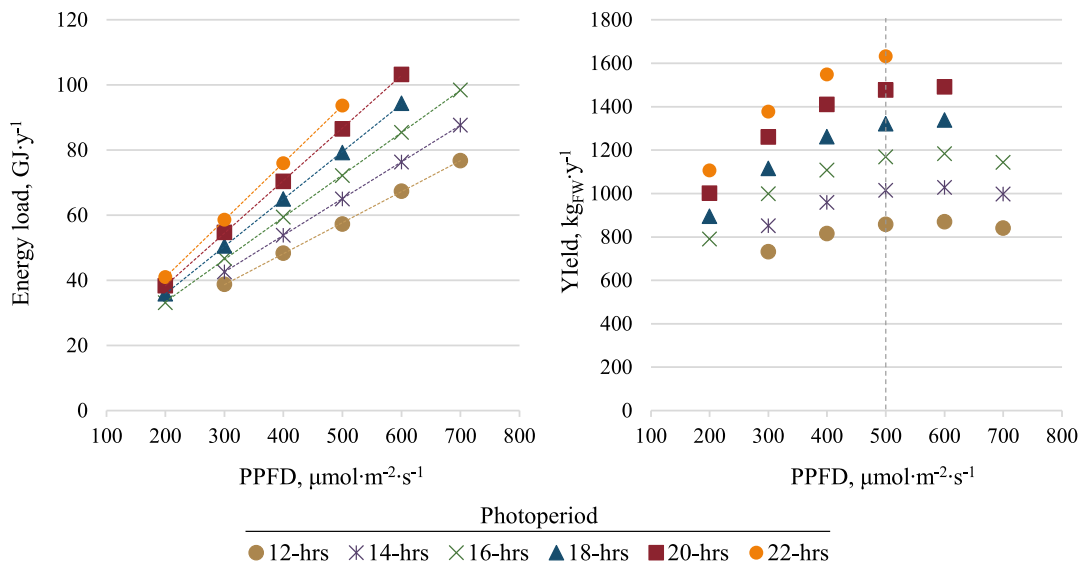


Fig. 10. Variation in annual energy load and yield with PPFD at an air temperature of 24 °C, VPD of 0.54 kPa, and photoperiods of 12 to 22 h.

Table 7

Resulting photoperiod (hours) for PPFD of 200 to 700 μmol·m⁻²·s⁻¹ combined to a DLI of 14, 18, 20, 22 and 24 mol·m⁻²·day⁻¹.

DLI, mol·m ⁻² ·d ⁻¹	PPFD, μmol·m ⁻² ·s ⁻¹	14	18	20	22	24
200		19.4	-	-	-	-
300		13.0	16.7	18.5	20.4	-
400		-	12.5	13.9	15.3	16.7
500		-	-	-	12.2	13.3
600		-	-	-	-	-
700		-	-	-	-	-

4. Discussion

The results obtained, the energy intensity, production intensity, and specific energy load of the scenarios at 24 °C and 0.54 kPa, are compared with data reported in the literature, as illustrated in Fig. 12. The additional data included are from two studies [3,19] that have estimated the energy load associated with space energy demands. It is important to specify that for a vertical farm with negligible heat exchanges through the building envelope, the impact of the size of the high-density CEA space has minimal impact under similar growing conditions. As an example, the numerically estimated annual energy load intensities for cooling and dehumidification were within 5% and 1%, respectively, for vertical farms having a footprint of 7.4 m² and 50,000 m² [27].

The energy intensity and production intensity estimated by Blom et al. [19] are respectively 22% and 44% lower than the corresponding

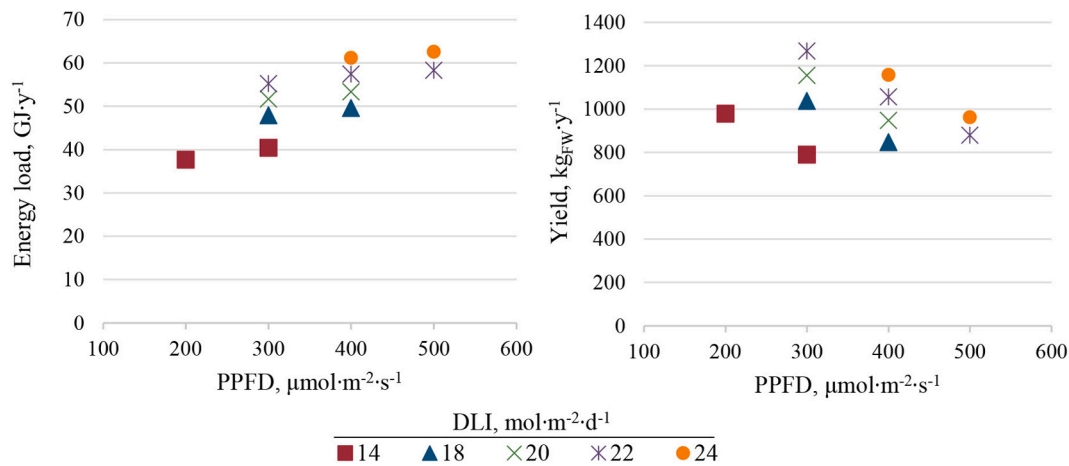


Fig. 11. Variation in annual energy load and yield with PPFD at an air temperature of 24 °C and VPD of 0.54 kPa for DLI of 14, 18, 20, 22 and 24 mol·m⁻²·d⁻¹.

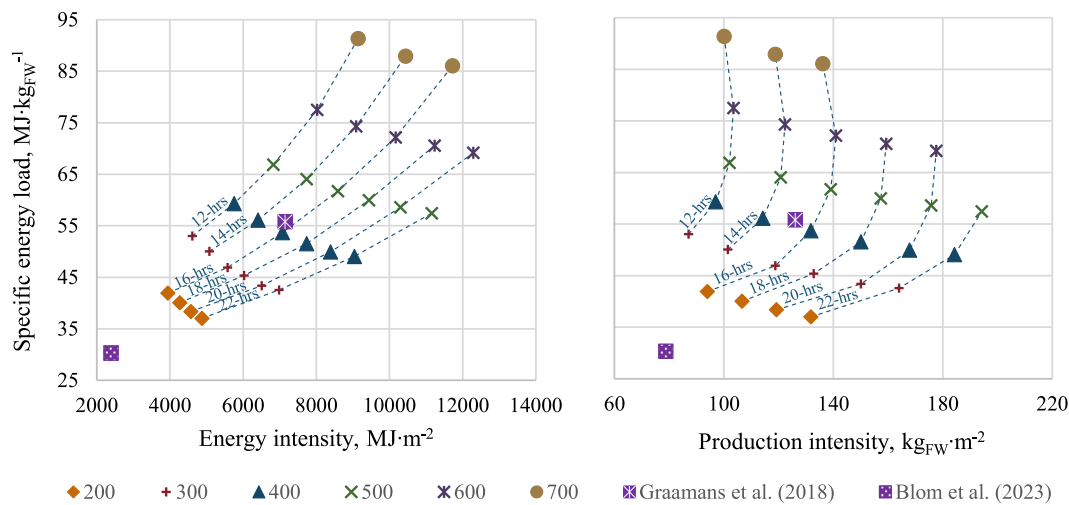


Fig. 12. Energy intensity, production intensity and specific energy load for the scenarios at 24 °C and 0.54 kPa and from other studies.

value for nearly identical growing conditions (24 °C / 0.54 kPa / 200 μmol·m⁻²·s⁻¹ / 16-h). The lower energy intensity from Blom et al. [19] is primarily attributed to using a higher PPE (3.5 vs 2.6 μmol·J⁻¹) and excluding energy load during the dark period. The results obtained using the proposed modelling approach estimated the energy load during the dark period to account for approximately 12% of the total energy load for this particular set of conditions. When considering all the modelled scenarios, the energy load during the dark period ranges from 1% to 19% of the total energy load. The lower production intensity is linked to the light productivity Blom et al. [19] used based on their operational conditions. Blom et al. [19] stated that higher production intensity could be achieved using light productivity data experimentally obtained by Carotti et al. [22].

The energy intensity and production intensity estimated by Graamans et al. [3] are respectively 15% lower and 25% higher than the nearest corresponding value for nearly identical growing conditions (28 °C / 0.54 kPa / 500 μmol·m⁻²·s⁻¹ / 16-h). The difference in energy intensity can be primarily attributed to temperature and VPD setpoints. In their study, floating setpoints allowed the air temperature and relative humidity to reach 30 °C and 90% (VPD of 0.42 kPa), reducing the energy load associated with cooling and dehumidification. Additionally, there are other differences in the energy modelling approach, as reported by Talbot and Monfet [27]. The discrepancy in production intensity is attributed to the growth model used by Graamans et al. [3], which tends to overestimate the growth rate in CEA applications, as

demonstrated by Talbot and Monfet [27].

The obtained yield in Section 3.4 for different combinations of PPFD and photoperiod, while maintaining a constant DLI, aligns with findings reported by Elkins and van Iersel [11], who observed an increase in shoot dry weight of 18% to 30% for DLI of 16 and 12 mol·m⁻²·d⁻¹, respectively, when the photoperiod was extended from 10 to 20 h. Similar results were reported by Kelly, Choe, Meng, and Runkle [12] for a DLI of 15.6 mol·m⁻²·d⁻¹, with dry weight increasing by 23–26%, depending on the cultivar when the PPFD is decreased by 90 μmol·m⁻²·s⁻¹. Additionally, they observed an increase in fresh weight of 18%–22% but also noted that at a lower DLI of 10.4 mol·m⁻²·d⁻¹, there was no difference in growth when changing the PPFD. This approach can potentially reduce the energy load while increasing the yield, reduce tip burn incidence and lower the purchase and installation cost of electric lighting with a low PPFD [35]. It also reduces the dehumidification load per fresh yield, which is noteworthy given that dehumidification units are typically less efficient than cooling units. Additionally, using electric lighting with a low PPFD decreases power demand, leading to potential cost savings. This is significant because, in many locations, electricity prices are often a combination of energy load and power demand.

5. Conclusion

This study assessed the annual energy load, distribution per category

and fresh yield for various growing conditions. It provided insight into the influence of the growing conditions on energy load and crop yield using a modelling approach, specifically focusing on energy load associated with space energy demands, excluding HVAC equipment. To improve energy efficiency, lowering the energy requirements through energy efficiency measures becomes as important as improving the energy performance of the HVAC equipment. The analysis presented in this study provides a comprehensive understanding of how growing conditions influence energy load and crop yield. The yield predicted with the model was compared and cross-referenced with existing literature. The key findings of the analysis can be summarised as follows:

- Most energy load can be attributed to lighting, which influences the demand for electricity and cooling. Both account for 50% to 87% of the energy load, with a noticeable increase as the PPFD rises. Consequently, for most scenarios, implementing energy efficiency measures such as improving PPE or implementing pulsing light strategies is crucial.
- Scenarios with a 24 °C air temperature resulted in higher energy load compared to scenarios at 20 °C and 28 °C. However, they also led to a substantial increase in crop yield, resulting in a consistent improvement in specific energy load.
- For most conditions, lowering the VPD setpoint is favourable as it reduces energy load without causing water stress that might hinder growth. Under certain conditions, notably at higher PPFD levels, changing the VPD no longer significantly influences energy load.
- At PPFD levels exceeding $500 \mu\text{mol}\cdot\text{m}^{-2}\cdot\text{s}^{-1}$, the results showed that growth was limited, while the energy load continued to increase linearly with PPFD.
- When maintaining a constant DLI, lowering the PPFD and extending the photoperiod reduced the energy load and significantly increased yield, resulting in a consistent improvement of the specific energy load. Additionally, this approach offers other advantages, such as lowering the cost of purchasing the lighting system and reducing the power demand of the space.
- Dehumidification is a highly energy-intensive process, but specific changes in the growing conditions consistently reduce its energy load. These include changing the temperature setpoint to 20 °C or 28 °C, reducing the VPD setpoint and decreasing the PPFD while extending the photoperiod for a constant DLI.

This study provided a better understanding of how growing

conditions influence energy load and crop yield. The results of this study or the energy modelling approach could be leveraged for implementing energy efficiency measures. However, it is essential to note that the dynamic crop model is still limited to lettuce cultivation under constant CO₂ concentration and for air temperatures of 20 °C, 24 °C and 28 °C. Future work would expand it to include other crops usually grown indoors, such as leafy greens, microgreens and strawberries.

CRediT authorship contribution statement

Marie-Hélène Talbot: Conceptualization, Software, Visualization, Methodology, Validation, Formal analysis, Writing – original draft.
Danielle Monfet: Methodology, Visualization, Writing – review & editing, Supervision, Funding acquisition.

Declaration of Generative AI and AI-assisted technologies in the writing process

While preparing this work, the authors used ChatGPT (GPT-3.5) to improve the language and readability of a few sentences (less than 10% of the text). After using this tool/service, the authors reviewed and edited the content as needed and took full responsibility for the publication's content.

Declaration of competing interest

The authors declare that they have no known competing financial interests or personal relationships that could have appeared to influence the work reported in this paper.

Data availability

Data will be made available on request.

Acknowledgements

This work was supported by the Fonds de Recherche du Québec – Nature et Technologies (Quebec, Canada), PhD scholarship for the first co-author, as well as NSERC Research grants RGPIN-2020-04576 and ALLRP 561361-21.

Appendix A. Appendix

Table 8

Parameters of the crop model.

Parameter	Description	Value	Interpolation method																			
$r_a, s \cdot m^{-1}$	Aerodynamic resistance	100 [32]	N/A																			
$r_s, s \cdot m^{-1}$	Stomatal resistance	$\frac{60 \cdot (1500 + PPFD)}{200 + PPFD}$ [32]	N/A																			
$c_\varepsilon, g \cdot J^{-1}$	Light use efficiency at a very high CO ₂ concentration	<table border="1"> <thead> <tr> <th rowspan="2">T_{ai}, °C</th> <th colspan="3">PPFD, μmol·m⁻²·s⁻¹</th> </tr> <tr> <th>200</th> <th>400</th> <th>750</th> </tr> </thead> <tbody> <tr> <td>20</td> <td>10.5324E-6</td> <td>10.5901E-6</td> <td>7.7421E-6</td> </tr> <tr> <td>24</td> <td>11.0025E-6</td> <td>11.6375E-6</td> <td>7.8226E-6</td> </tr> <tr> <td>28</td> <td>10.7513E-6</td> <td>9.5993E-6</td> <td>6.9296E-6</td> </tr> </tbody> </table> <p>Calibrated values by Talbot and Monfet [27]</p>	T _{ai} , °C	PPFD, μmol·m ⁻² ·s ⁻¹			200	400	750	20	10.5324E-6	10.5901E-6	7.7421E-6	24	11.0025E-6	11.6375E-6	7.8226E-6	28	10.7513E-6	9.5993E-6	6.9296E-6	Second-degree polynomial regression
T _{ai} , °C	PPFD, μmol·m ⁻² ·s ⁻¹																					
	200	400	750																			
20	10.5324E-6	10.5901E-6	7.7421E-6																			
24	11.0025E-6	11.6375E-6	7.8226E-6																			
28	10.7513E-6	9.5993E-6	6.9296E-6																			
$k_{s,el}$	Extinction coefficient of lettuces	0.66 Calibrated values by Talbot and Monfet [27]	N/A																			
$c_{gr,max}, s^{-1}$	Saturation growth rate at 20°C	<table border="1"> <thead> <tr> <th rowspan="2">T_{ai}, °C</th> <th colspan="3">PPFD, μmol·m⁻²·s⁻¹</th> </tr> <tr> <th>200</th> <th>400</th> <th>750</th> </tr> </thead> <tbody> <tr> <td>20</td> <td>7.576E-7</td> <td>10.474E-7</td> <td>11.433E-7</td> </tr> <tr> <td>24</td> <td>6.715E-7</td> <td>8.733E-7</td> <td>8.988E-7</td> </tr> <tr> <td>28</td> <td>1.764E-7</td> <td>4.679E-7</td> <td>5.264E-7</td> </tr> </tbody> </table> <p>Calibrated values by Talbot and Monfet [27]</p>	T _{ai} , °C	PPFD, μmol·m ⁻² ·s ⁻¹			200	400	750	20	7.576E-7	10.474E-7	11.433E-7	24	6.715E-7	8.733E-7	8.988E-7	28	1.764E-7	4.679E-7	5.264E-7	Second-degree polynomial regression
T _{ai} , °C	PPFD, μmol·m ⁻² ·s ⁻¹																					
	200	400	750																			
20	7.576E-7	10.474E-7	11.433E-7																			
24	6.715E-7	8.733E-7	8.988E-7																			
28	1.764E-7	4.679E-7	5.264E-7																			
c_β	Yield factor indicating the respiratory and synthesis losses of non-structural material due to growth	<table border="1"> <thead> <tr> <th rowspan="2">T_{ai}, °C</th> <th colspan="3">PPFD, μmol·m⁻²·s⁻¹</th> </tr> <tr> <th>200</th> <th>400</th> <th>750</th> </tr> </thead> <tbody> <tr> <td>20</td> <td>0.401</td> <td>0.402</td> <td>0.403</td> </tr> <tr> <td>24</td> <td>0.400</td> <td>0.400</td> <td>0.402</td> </tr> <tr> <td>28</td> <td>0.425</td> <td>0.404</td> <td>0.403</td> </tr> </tbody> </table> <p>Calibrated values by Talbot and Monfet [27]</p>	T _{ai} , °C	PPFD, μmol·m ⁻² ·s ⁻¹			200	400	750	20	0.401	0.402	0.403	24	0.400	0.400	0.402	28	0.425	0.404	0.403	Linear
T _{ai} , °C	PPFD, μmol·m ⁻² ·s ⁻¹																					
	200	400	750																			
20	0.401	0.402	0.403																			
24	0.400	0.400	0.402																			
28	0.425	0.404	0.403																			
SLA, cm ² ·gdw ⁻¹	Specific leaf area	<table border="1"> <thead> <tr> <th rowspan="2">T_{ai}, °C</th> <th colspan="3">PPFD, μmol·m⁻²·s⁻¹</th> </tr> <tr> <th>200</th> <th>400</th> <th>750</th> </tr> </thead> <tbody> <tr> <td>20</td> <td>327</td> <td>261</td> <td>218</td> </tr> <tr> <td>24</td> <td>452</td> <td>365</td> <td>272</td> </tr> <tr> <td>28</td> <td>400</td> <td>314</td> <td>250</td> </tr> </tbody> </table> <p>Extracted from Carotti et al. [22] experiments</p>	T _{ai} , °C	PPFD, μmol·m ⁻² ·s ⁻¹			200	400	750	20	327	261	218	24	452	365	272	28	400	314	250	Second-degree polynomial regression
T _{ai} , °C	PPFD, μmol·m ⁻² ·s ⁻¹																					
	200	400	750																			
20	327	261	218																			
24	452	365	272																			
28	400	314	250																			
DW _{content} , %	Dry weight content at harvest	<table border="1"> <thead> <tr> <th colspan="3">PPFD, μmol·m⁻²·s⁻¹</th> </tr> <tr> <th>200</th> <th>400</th> <th>750</th> </tr> </thead> <tbody> <tr> <td>2.6</td> <td>3.8</td> <td>4.2</td> </tr> </tbody> </table> <p>Extracted from Carotti et al. [22] experiments</p>	PPFD, μmol·m ⁻² ·s ⁻¹			200	400	750	2.6	3.8	4.2	Second-degree polynomial regression										
PPFD, μmol·m ⁻² ·s ⁻¹																						
200	400	750																				
2.6	3.8	4.2																				

Appendix B. Supplementary data

Supplementary data to this article can be found online at <https://doi.org/10.1016/j.apenergy.2024.123406>.

References

- [1] Shahbandeh M. Global vertical farming market projection 2022–2032. 2023.
- [2] Kozai T. Why LED lighting for urban agriculture? LED lighting for urban agriculture. Springer; 2016. p. 3–18.
- [3] Graamans L, Baeza E, van den Dobbelen A, Tsafaras I, Stanghellini C. Plant factories versus greenhouses: comparison of resource use efficiency. *Agr Syst* 2018; 160:31–43.
- [4] Eaton M, Shelford T, Cole M, Mattson N. Modeling resource consumption and carbon emissions associated with lettuce production in plant factories. *J Clean Prod* 2023;384:135569.
- [5] Talbot M-H, Monfet D, Lalonde T, Haillod D. Impact of Modelling Thermal Phenomena in a High-Density Controlled Environment Agriculture (CEA-HD) Space. *Building Simulation* 2021. Bruges. 2021.
- [6] Hoyt T, Arens E, Zhang H. Extending air temperature setpoints: simulated energy savings and design considerations for new and retrofit buildings. *Build Environ* 2015;88:89–96.
- [7] Carotti L, Graamans L, Puksic F, Butturini M, Meinen E, Heuvelink E, et al. Plant factories are heating up: hunting for the best combination of light intensity, air temperature and root-zone temperature in lettuce production. *Front Plant Sci* 2021;11:592171.
- [8] Kozai T, Niu G, Takagaki M. Plant factory: An indoor vertical farming system for efficient quality food production. Academic Press; 2015.
- [9] Jung DH, Kim D, Yoon HI, Moon TW, Park KS, Son JE. Modeling the canopy photosynthetic rate of romaine lettuce (*Lactuca sativa* L.) grown in a plant factory at varying CO₂ concentrations and growth stages. *Horticult Environ Biotechnol* 2016;57:487–92.
- [10] Jin W, Formiga Lopez D, Heuvelink E, Marcelis LFM. Light use efficiency of lettuce cultivation in vertical farms compared with greenhouse and field. *Food Energy Security* 2023;12:e391.
- [11] Elkins C, van Iersel MW. Longer photoperiods with the same daily light integral increase daily electron transport through photosystem II in lettuce. *Plants (Basel)* 2020:9.
- [12] Kelly N, Choe D, Meng Q, Runkle ES. Promotion of lettuce growth under an increasing daily light integral depends on the combination of the photosynthetic photon flux density and photoperiod. *Sci Hortic* 2020;272:109565.
- [13] EPRI. Indoor agriculture : A utility, water, sustainability, technology and market overview. 2018.
- [14] Holden NM, Wolfe ML, Ogejo JA, Cummins EJ. Introduction to Biosystems engineering. ASABE and Virginia Tech Publishing; 2021.
- [15] Ohyama K, Yamaguchi J, Enjoji A. Evaluating labor productivity in a plant production system with sole-source lighting: a case study. *Hort Technol Hort* 2018;28:121–8.
- [16] Blom T, Jenkins A, Pulselli RM, van den Dobbelen AAJF. The embodied carbon emissions of lettuce production in vertical farming, greenhouse horticulture, and open-field farming in the Netherlands. *J Clean Prod* 2022:377.

- [17] Talbot M-H, Lalonde T, Beaulac A, Haillot D, Monfet D. Comparing the energy performance of different controlled environment agriculture spaces using TRNSYS. *eSim* 2022. Ottawa. 2022.
- [18] Zhang Y, Kacira M. Comparison of energy use efficiency of greenhouse and indoor plant factory system. *Europ J Horticult Sci* 2020;85:310–20.
- [19] Blom T, Jenkins A, van den Dobbelsteen A. Synergetic integration of vertical farms and buildings: reducing the use of energy, water, and nutrients. *Front Sustain Food Syst* 2023:7.
- [20] Stanghellini C, Katzin D. The dark side of lighting: A critical analysis of vertical farms' environmental impact. 2023.
- [21] Eaton M, Shelford T, Cole M, Mattson N. Modeling resource consumption and carbon emissions associated with lettuce production in plant factories. *J Clean Prod* 2023:384.
- [22] Carotti L, Graamans L, Puksic F, Butturini M, Meinen E, Heuvelink E, et al. Plant factories are heating up: hunting for the best combination of light intensity, air temperature and root-zone temperature in lettuce production. *Front Plant Sci* 2021;11.
- [23] Sabeh NC, Ross D, Miner L, Everett S. Literature review of energy and water use in controlled environment horticulture and potential efficiency opportunities. Pacific Gas Electric Company 2022.
- [24] Weidner T, Yang A, Hamm MW. Energy optimisation of plant factories and greenhouses for different climatic conditions. *Energ Conver Manage* 2021;243: 114336.
- [25] Ahamed MS, Sultan M, Monfet D, Rahman MS, Zhang Y, Zahid A, et al. A critical review on efficient thermal environment controls in indoor vertical farming. *J Clean Prod* 2023;425:138923.
- [26] Van Henten EJ. Validation of a dynamic lettuce growth model for greenhouse climate control. *Agr Syst* 1994;45:55–72.
- [27] Talbot M-H, Monfet D. Development of a crop growth model for the energy analysis of controlled agriculture environment spaces. *Biosyst Eng* 2024;238: 38–50.
- [28] Talbot M-H, Monfet D. Estimating the impact of crops on peak loads of a building-integrated agriculture space. *Sci Technol Built Environ* 2020;26:1448–60.
- [29] Ahamed MS, Sultan M, Monfet D, Rahman MS, Zhang Y, Zahid A, et al. A critical review on efficient thermal environment controls in indoor vertical farming. *J Clean Prod* 2023:425.
- [30] Jans-Singh M, Ward R, Choudhary R. Co-simulating a greenhouse in a building to quantify co-benefits of different coupled configurations. *J Build Perform Simul* 2021;14:247–76.
- [31] Klein SA, al. e.. TRNSYS 18: A transient system simulation program. Madison, WI, USA: Solar Energy Laboratory, University of Wisconsin; 2017.
- [32] Graamans L, van den Dobbelsteen A, Meinen E, Stanghellini C. Plant factories; crop transpiration and energy balance. *Agr Syst* 2017;153:138–47.
- [33] Pennisi G, Orsini F, Landolfo M, Pistillo A, Crepaldi A, Nicola S, et al. Optimal photoperiod for indoor cultivation of leafy vegetables and herbs. 2020.
- [34] Silva LM, Cruz LP, Pacheco VS, Machado EC, Purquerio LFV, Ribeiro RV. Energetic efficiency of biomass production is affected by photoperiod in indoor lettuce cultivation. *Theoret Exp Plant Physiol* 2022;34:265–76.
- [35] Kelly N, Meng Q, Runkle ES. Photoperiod, light intensity and daily light intergral. *Produce Grower* 2022:16–9.